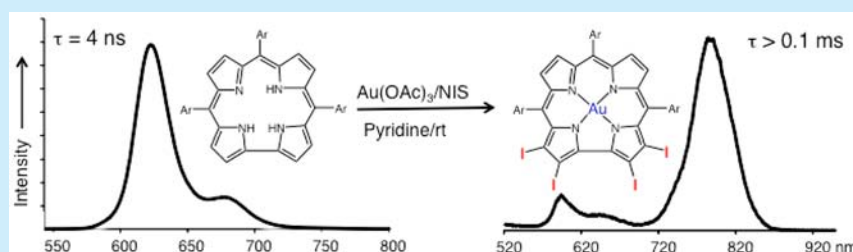


## One-Pot Conversion of Fluorophores to Phosphorophores

Matan Soll,<sup>†,§</sup> Kolanu Sudhakar,<sup>†,§</sup> Natalia Fridman,<sup>†</sup> Alexander Müller,<sup>‡</sup> Beate Röder,<sup>‡</sup> and Zeev Gross<sup>\*,†,§</sup><sup>†</sup>Schulich Faculty of Chemistry, Technion - Israel Institute of Technology, Haifa 32000, Israel<sup>‡</sup>AG Photobiophysik, Humboldt-Universität zu Berlin MNF, Newtonstrass, 1512489 Berlin, Germany

## S Supporting Information



**ABSTRACT:** Facile, one-pot conversion of free base 5,10,15-tris(pentafluorophenyl)corrole, (H<sub>3</sub>)tpfc, into the coinage metal complexes of 2,3,17,18-tetraiodo-5,10,15-tris(pentafluorophenyl)corrole, (I<sub>4</sub>-tpfc)M (M = Cu, Ag, Au), is reported. The iodination/metalation procedures provide much higher yields and larger selectivity than both conceivable stepwise syntheses. Photophysical analysis shows that the gold(III) complex (I<sub>4</sub>-tpfc)Au displays phosphorescence at room temperature and a substantial quantum yield for singlet oxygen formation.

The development of chromophores that efficiently absorb visible light, display long-lived excited states, and emit at the far-red end of the spectrum is of great importance for many applications, including light-emitting diodes (LED),<sup>1,2</sup> sensing of oxygen and other gaseous molecules, bioimaging,<sup>3,4</sup> and more. The vast majority of compounds that fulfill the above requirements are based on complexes with the most rare metals such as platinum and iridium, thus limiting their utility. This is also true for the first reported phosphorescent corrole complexes, (tpfc)Ir, (tpfc)Au, and (tpfc)Rh, where tpfc stands for the trianion of 5,10,15-tris(pentafluorophenyl)corrole, (H<sub>3</sub>)-tpfc.<sup>5–9</sup> More recently, we have decided to introduce the heavy atom effect via covalent C–I bonds on the corrole skeleton rather than relying on heavy and expensive metal ions.<sup>11</sup> In line with that, we have performed iodination on the aluminum, gallium, and phosphorus complexes (M = Al, Ga, P(OH)<sub>2</sub>, in (tpfc)M), which led to successful preparation of the corresponding complexes of 2,3,17,18-tetraiodo-5,10,15-tris(pentafluorophenyl)corrole (I<sub>4</sub>-tpfc)M and 2,3,17-trisiodo-5,10,15-tris(pentafluorophenyl)corrole (I<sub>3</sub>-tpfc)M.<sup>10</sup> Spectroscopic examinations indicated that this kind of complexes, and to some extent those of octabrominated corroles, display prompt fluorescence, phosphorescence, and delayed thermal fluorescence, all at room temperature.<sup>10,12–17</sup>

To generalize the above approach, we tried to obtain iodinated free base corrole by treating (H<sub>3</sub>)tpfc with *N*-iodosuccinimide (NIS) or molecular iodine in a methanol solution, exactly as previously performed for its corresponding metal complexes.<sup>10,16</sup> NMR examination of the thus-obtained main product revealed it to be nonaromatic (Figure S1). A more in-depth characterization was, however, not performed because of the limited stability of

that compound. The next attempt was to perform the iodination reactions in pyridine as solvent, considering that the bromine/pyridine complex is a very good brominating agent<sup>18,19</sup> and existing evidence for formation of iodine/pyridine complexes.<sup>19,20</sup> Indeed, treatment of a pyridine solution of (H<sub>3</sub>)tpfc by NIS yielded 2,3,17,18-tetraiodo-5,10,15-tris(pentafluorophenyl)corrole, (H<sub>3</sub>)(I<sub>4</sub>-tpfc), in a reasonable 40% yield. Confirmation about the selective iodination of only the directly connected pyrrole subunits was achieved by NMR analyses (Figure S2) that disclosed the C<sub>2</sub> symmetry axis therein; and via X-ray crystallography of the corresponding metal chelates. The successful synthesis of the iodinated free-base corrole allowed for accessing the corresponding transition-metal complexes, of which the choice was to focus on the group 11 triad. The Cu, Ag, and Au complexes of both (H<sub>3</sub>)tpfc and (H<sub>3</sub>)(I<sub>4</sub>-tpfc) were prepared for obtaining a meaningful series of compounds that might differentiate between the effects of the iodine atoms and the chelated metal on the physical properties.

Three strategies were employed for the synthesis of the desired (I<sub>4</sub>-tpfc)M complexes with M = Cu, Ag, and Au: (a) iodination of (H<sub>3</sub>)tpfc, followed by metalation of (H<sub>3</sub>)(I<sub>4</sub>-tpfc); (b) metalation of (H<sub>3</sub>)tpfc, followed by iodination of the (tpfc)M complexes; and (c) a one-pot metalation/iodination procedure applied on (H<sub>3</sub>)tpfc (Figure 1). The main drawback of the first option is that the iodinated free-base corrole is obtained in 40% yield only. Regarding the second approach, one severe limitation is that insertion of gold into (H<sub>3</sub>)tpfc proceeds in low and highly

Received: September 23, 2016

Published: November 10, 2016

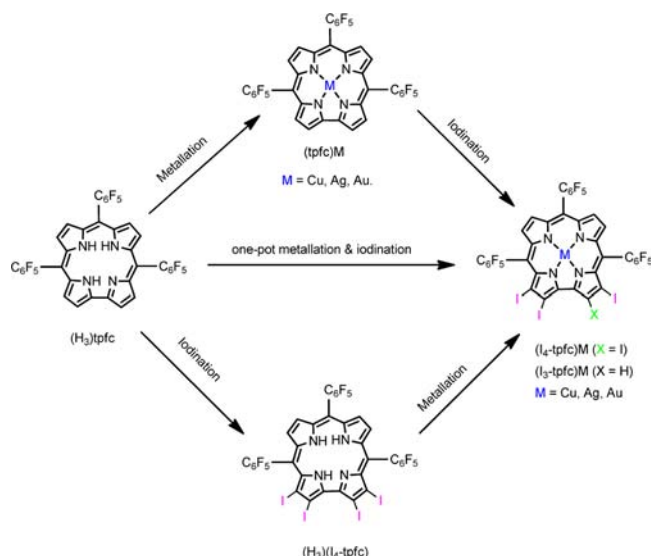


**Figure 1.** Three approaches for the synthesis of group 11 metal complexes of  $\beta$ -pyrrole-iodinated corroles.

variable yields.<sup>9a,b</sup> In addition, iodination might proceed with different selectivity for each of the applied (tpfc)M complexes.

The first strategy proved to be quite beneficial regarding reaction times and the respectable metalation yields. (H<sub>3</sub>)(I<sub>4</sub>-tpfc) (1 equiv) was stirred in pyridine with Cu(OAc)<sub>2</sub> (10 equiv), AgOAc (5 equiv), or Au(OAc)<sub>3</sub> (2 equiv) at room temperature under ambient conditions to yield (I<sub>4</sub>-tpfc)Cu, (I<sub>4</sub>-tpfc)Ag, and (I<sub>4</sub>-tpfc)Au, respectively. For this two-step procedure, the overall yields relative to (H<sub>3</sub>)tpfc were 36%, 26.8%, and 28.8%, respectively. For the other stepwise synthesis, pyridine solutions of (H<sub>3</sub>)tpfc (1 equiv) were treated with either Cu(OAc)<sub>2</sub> (10 equiv, 2 h, rt) or Ag(OAc) (3 equiv, 12 h, reflux), or Au(OAc)<sub>3</sub> (2 equiv, 24 h, reflux) to yield (tpfc)Cu, (tpfc)Ag, and (tpfc)Au in 91%, 60%, and 8% yield, respectively. Iodination of the isolated (tpfc)M complexes was performed at rt for either 1 h (M = Cu and Au) or 12 h (M = Ag). The main product in the case of copper was (I<sub>4</sub>-tpfc)Cu, while the tris-iodinated complexes dominated for silver and gold yielding (I<sub>3</sub>-tpfc)Ag and (I<sub>3</sub>-tpfc)Au. The overall yields relative to (H<sub>3</sub>)tpfc were 63.7%, 33%, and 4.16%, respectively. One main conclusion from the comparison between the two kinds of two-step procedures is that metal insertion proceeds under milder conditions and provides larger chemical yields for (H<sub>3</sub>)(I<sub>4</sub>-tpfc) than for (H<sub>3</sub>)tpfc, particularly in the case of gold. This is reminiscent of observations regarding auration of other β-pyrrole-substituted corroles.<sup>9b-d</sup>

Based on the acquired knowledge, the in situ iodination/metalation procedure was explored. Pleasingly, the results were very good. Pyridine solutions composed of  $(\text{H}_3)\text{tpfc}$  (1 equiv), NIS (10 equiv), and either one of the metal salts  $\text{Cu}(\text{OAc})_2$  (10 equiv),  $\text{AgOAc}$ , or  $\text{Au}(\text{OAc})_3$  (2 equiv in each case) yielded the corresponding tetraiodinated metal complexes  $(\text{I}_4\text{-tpfc})\text{Cu}$ ,  $(\text{I}_4\text{-tpfc})\text{Ag}$ , and  $(\text{I}_4\text{-tpfc})\text{Au}$  in yields of 76%, 45%, and 53%, respectively, within 1–6 h under ambient reaction conditions (SI).

The comparison between the one-pot synthesis vs the two stepwise approaches is summarized in [Figure 2](#). The first notable aspects are that prior metalation of (H<sub>3</sub>)tpfc by silver and gold requires long heating and that the sequential iodination leads to the tris- rather than the tetraiodinated complexes. In the opposite

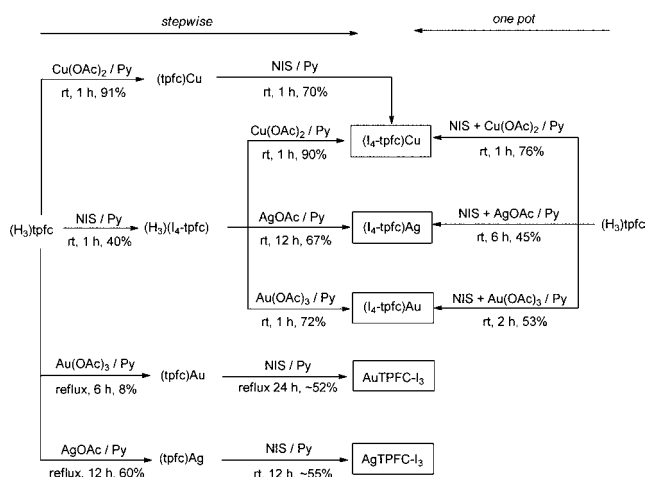


**Figure 2.** Comparison of chemical yields and the identity of the main product in the stepwise approaches and the one-pot procedure for the synthesis of iodinated-corrole chelates of copper, silver, and gold.

approach, the selectivity to the tetraiodinated corrole is larger, and the reaction conditions for metalation are much milder. This suggests that the one-pot procedure starts with iodination followed by formation of the more stable metal complexes. As an outcome, this methodology ends up being more facile in terms of reaction conditions and time, more selective to the tetraiodinated complexes, and of higher overall yields 76% vs 36–64% for copper, 45% vs 27% for Ag, and 53% vs 29% for Au.

Crystal structures obtained for the three (I<sub>4</sub>-tpfc)M complexes (Figure 3) revealed that all are neutral, and each features a 4-

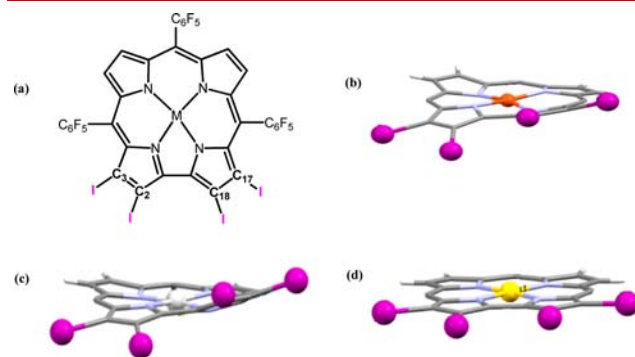


**Figure 3.** Drawing of the (I<sub>4</sub>-tpfc)M complexes with the numbering of the substituted C atoms (a) and side views (with the *meso*-C<sub>6</sub>F<sub>5</sub> groups omitted for clarity) of the X-ray-determined molecular structures of (I<sub>4</sub>-tpfc)Cu (b), (I<sub>4</sub>-tpfc)Ag (c), and (I<sub>4</sub>-tpfc)Au (d).

coordinate metal ion,<sup>21</sup> consistent with expectations for the formal d<sup>8</sup> + 3 oxidation state therein. There are, however, distinct differences in the degree of planarity of the macrocycle: large deformation in the case of copper, somewhat less so for silver, while the gold complex is almost perfectly planar. This is manifested by the angles measured between the plane defined by the 4 N atoms and the I–C–C–I units of the two iodinated pyrrole moieties, as well as by the angles between the two latter (Table 1). The reason for this remarkable differences has been previously deduced by Ghosh et al. to be due to an increase in the redox-innocence of (corrolo)M complexes upon moving from Cu to Ag and finally to Au.<sup>9c</sup>

All of the examined iodinated corroles exhibited typical near-UV Soret band and far-visible Q bands ([Figure S22](#) and [Table](#)

Table 1. Selected Structural Data for Demonstrating the Remarkable Differences between the Gold and the Silver/Copper Complexes

entry	deviation from the N <sub>4</sub> plane (Å)		dihedral angle (Å) between I–C–C–I planes
	I–C <sub>2</sub> –C <sub>3</sub> –I plane	I–C <sub>17</sub> –C <sub>18</sub> –I plane	
(I <sub>4</sub> -tpfc)Cu	19.60	20.35	34.15
(I <sub>4</sub> -tpfc)Ag	14.86	22.56	32.19
(I <sub>4</sub> -tpfc)Au	3.03	3.96	6.57

S2), with significant red shifts relative to (H<sub>3</sub>)tpfc and the (tpfc)M complexes: 8, 11, 8, and 6 nm for the Soret band and 58, 24, 17, and 19 nm for the lowest energy Q-band of (H<sub>3</sub>)(I<sub>4</sub>-tpfc), (I<sub>4</sub>-tpfc)Cu, (I<sub>4</sub>-tpfc)Ag, and (I<sub>4</sub>-tpfc)Au, respectively. Shifts in the UV–vis spectra of porphyrins and corroles are not easy to analyze because they are sensitive to both electronic and structural variations.<sup>17,22</sup> Nevertheless, the red shifts obtained for the almost perfectly planar (I<sub>4</sub>-tpfc)Au is reminiscent of nondistorted octabrominated metalcorroles where the HOMO–LUMO gap was found to decrease due the addition of electron withdrawing groups on the macrocycle periphery.<sup>10,12–17,23,24</sup> The major expected effect of replacing C–H by C–I bonds is reduced fluorescence intensity because of several aspects: (a) an increase of nonradiative decay rates due to the weaker C–I bonds; (b) additional nonradiative decay channels if the macrocycle becomes more distorted; and (c) an increased intersystem probability due to the heavy atom effect.<sup>10,11</sup> Indeed, all of the iodinated corroles displayed heavily quenched fluorescence intensity relative to (H<sub>3</sub>)tpfc (Figures S23 and S24(b)). On the other hand, only the gold(III) complexes (tpfc)Au and (I<sub>4</sub>-tpfc)Au displayed phosphorescence (vide infra) at room temperature. This is clearly related to their much larger structural rigidity relative to the corresponding copper and silver corroles.<sup>8,9</sup> We may hence conclude that macrocycle deformation must be prevented for turning fluorophores into phosphorophores via heavy atom substitution. This conclusion is further supported by the recently reported phosphorescence of the aluminum, gallium, and phosphorus chelates of iodinated corroles, in all of which the macrocycle is remarkably planar.<sup>10,16,17</sup>

The most straightforward indication for long-lived photo-excited states is found by recording the emission spectrum long after the excited singlet states decayed (<1–5 ns). Parts a–c of Figures 4 display the emission spectra of (tpfc)Au and (I<sub>4</sub>-tpfc)Au, obtained after a 100 μs postexcitation delay. This is clearly indicative of a decay from long-lived triplet states, a conclusion that was further supported by the large Stokes shift for (I<sub>4</sub>-tpfc)Au ( $\lambda_{\text{max(abs)}}$  = 583 nm,  $\lambda_{\text{max(emission)}}$  = 787 nm) and the effective quenching under an oxygen atmosphere. Interestingly, much more intense phosphorescence is detectable when (I<sub>4</sub>-tpfc)Au is excited at the Q-band maximum of 583 nm rather than at the Soret maximum of 421 nm, despite of the 5-fold smaller optical density of the former.

The effective emission quenching under aerobic conditions suggests that these complexes could activate triplet oxygen. This was checked for the full series by looking at time-dependent changes at 1270 ± 15 nm, the characteristic  $\lambda_{\text{max}}$  of singlet oxygen phosphorescence. The data presented in Figure 5 and Table 2 clearly show that only (H<sub>3</sub>)tpfc, (tpfc)Au, H<sub>3</sub>(I<sub>4</sub>-tpfc), and (I<sub>4</sub>-tpfc)Au catalyze <sup>1</sup>O<sub>2</sub> formation. This is consistent with the absence of any detectable long-lived triplet-excited states for the rest of the series. For the (H<sub>3</sub>)(I<sub>4</sub>-tpfc) signal fit, a strong photosensitizer phosphorescence had to be taken into account (approximately a factor of 2 in relative amplitude) via an

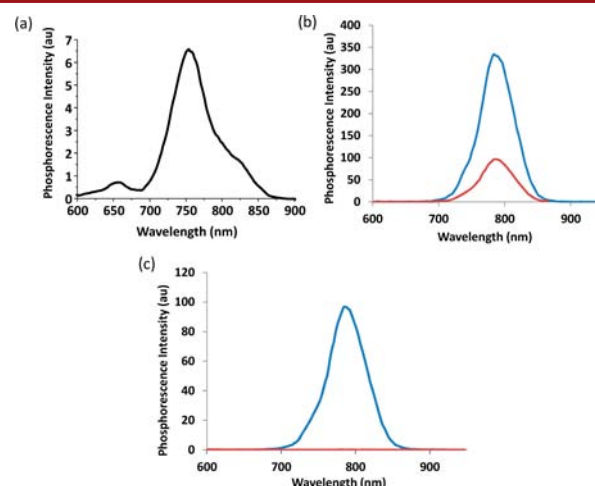


Figure 4. Phosphorescence detected under anaerobic conditions and 0.1 ms post excitation for: (a) (tpfc)Au with excitation at 420 nm; (b) of the same (I<sub>4</sub>-tpfc)Au sample, but by excitation of the Soret band (421 nm, red line) and the Q-band (581 nm, blue line); (c) of (I<sub>4</sub>-tpfc)Au under anaerobic conditions (blue line) and after exposure to O<sub>2</sub> (red line).

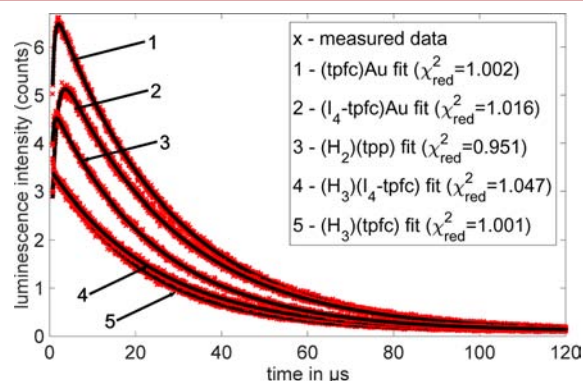


Figure 5. Time-resolved <sup>1</sup>O<sub>2</sub> signal intensities in toluene. Fits of the data were conducted following the standard biexponential model for singlet oxygen kinetics.<sup>26</sup> The goodness of the fit is indicated by the reduced  $\chi^2$ -test. The concentrations were adjusted for an optical density of 0.241 ± 0.003 at 405 nm (excitation wavelength of this measurement) in order to estimate a relative singlet oxygen quantum yield.

additional exponential decay in the standard biexponential singlet oxygen decay model.<sup>25</sup> (H<sub>3</sub>)tpfc and H<sub>3</sub>(I<sub>4</sub>-tpfc) displayed similar singlet oxygen formation quantum yields, 0.7 ± 0.1 relative to 5,10,15,20-tetraphenylporphyrin, while (tpfc)Au and (I<sub>4</sub>-tpfc)Au displayed quantum yields of 0.4 ± 0.1 and 1.5 ± 0.2, respectively. (I<sub>4</sub>-tpfc)Au also displayed the longest triplet state lifetime in the presence of oxygen, 1.2 ± 0.1 μs, which apparently accounts for its high quantum yield. Although (H<sub>3</sub>)tpfc and (H<sub>3</sub>)(I<sub>4</sub>-tpfc) exhibited reasonable singlet oxygen formation yields, they also bleached quite fast. In contrast, both (tpfc)Au and (I<sub>4</sub>-tpfc)Au did exhibit very high photostability.



Table 2. Photophysical Properties of All of the Corrole Series<sup>a</sup>

entry	$T_{\Delta}$ ( $^1\text{O}_2$ meas) ( $\mu\text{s}$ )	$T_{\text{T}}$ ( $^1\text{O}_2$ meas) ( $\mu\text{s}$ )	$T_{\text{T}}$ (LFPL meas) ( $\mu\text{s}$ )	$\Phi_{\Delta}/\Phi_{\Delta}(\text{TPP})$	$\Phi_{\text{FI}}/\Phi_{\text{FI}}(\text{TPP})$
(H <sub>3</sub> )tpfc	22 ± 1	0.3 ± 0.1	0.2 ± 0.1	0.7 ± 0.1	1.2 ± 0.1
(H <sub>3</sub> )(I <sub>4</sub> -tpfc)	25 ± 1	0.3 ± 0.1	0.3 ± 0.1	0.7 ± 0.1	<0.01
(tpfc)Au	27 ± 1	0.5 ± 0.1	0.4 ± 0.1	0.4 ± 0.1	<0.01
(I <sub>4</sub> -tpfc)Au	27 ± 1	1.2 ± 0.1	1.2 ± 0.1	1.5 ± 0.2	<0.01
(tpfc)Cu				<0.01	<0.01
(I <sub>4</sub> -tpfc)Cu				<0.01	<0.01
(tpfc)Ag				<0.01	<0.01
(I <sub>4</sub> -tpfc)Ag				<0.01	<0.01
(H <sub>2</sub> )tpp (ref)	24 ± 1	0.3 ± 0.1	0.3 ± 0.1	1.0 ± 0.1	1.0 ± 0.1

<sup>a</sup> $\Phi_{\Delta}$  is singlet oxygen quantum yield,  $\Phi_{\text{FI}}$  is fluorescence quantum yield,  $\tau_{\text{T}}$  is triplet lifetime, and  $\tau_{\Delta}$  is singlet oxygen lifetime.

We introduce a very efficient and facile one-pot synthesis of group 11 metals with tetraiodinated corroles. By doing so, the intense fluorophore (H<sub>3</sub>)tpfc may be converted into novel phosphorophores. Both C–H/C–I substitution on the macrocycle and insertion of transition metal ions into the N4 coordination core increase the singlet to triplet ISC probability, but reasonable phosphorescence and singlet oxygen formation is only achieved when metalation does not induce macrocycle deformation. The complex that was found to meet all the above criteria is (I<sub>4</sub>-tpfc)Au, which displays the strongest phosphorescence intensity and is also the best catalyst for the photoinduced formation of singlet oxygen. We trust the conclusions deduced from this research to be of great use for structure/activity tuning of other corroles and related ligands.

## ■ ASSOCIATED CONTENT

### Supporting Information

The Supporting Information is available free of charge on the ACS Publications website at DOI: [10.1021/acs.orglett.6b02877](https://doi.org/10.1021/acs.orglett.6b02877).

Experimental section; <sup>1</sup>H, <sup>19</sup>F NMR, HRMS, absorption, and emission spectra (PDF)

Crystallographic data (I<sub>4</sub>-tpfc)Cu (CIF)

Crystallographic data (I<sub>4</sub>-tpfc)Ag (CIF)

Crystallographic data (I<sub>4</sub>-tpfc)Au (CIF)

Crystallographic data (tpfc)Au (CIF)

## ■ AUTHOR INFORMATION

### Corresponding Author

\*E-mail: [chr10zg@tx.technion.ac.il](mailto:chr10zg@tx.technion.ac.il).

### Author Contributions

§M.S. and K.S. contributed equally.

### Notes

The authors declare no competing financial interest.

## ■ ACKNOWLEDGMENTS

This research was supported by a grant to Z.G. by the Pazy Foundation. A.M. thanks the land Berlin for financial support from the “Elsa-Neumann-Stipendium”.

## ■ REFERENCES

- Xiang, H.; Cheng, J.; Ma, X.; Zhou, X.; Chruma, J. J. *Chem. Soc. Rev.* **2013**, *42*, 6128–6185.
- Yersin, H., Ed. *Highly Efficient OLEDs with Phosphorescent Materials*; Wiley-VCH: Weinheim, 2008.
- Zhao, Q.; Huang, C.; Li, F. *Chem. Soc. Rev.* **2011**, *40*, 2508–2524.
- Bunzli, J. C. G. *Chem. Rev.* **2010**, *110*, 2729–2755.

(5) Alemayehu, A. B.; Day, N. U.; Mani, T.; Rudine, A. B.; Thomas, K. E.; Gederaas, O. A.; Vinogradov, S. A.; Wamser, C. C.; Ghosh, A. *ACS Appl. Mater. Interfaces* **2016**, *8*, 18935–18942.

(6) Palmer, J. H.; Durrell, A. C.; Gross, Z.; Winkler, J. R.; Gray, H. B. *J. Am. Chem. Soc.* **2010**, *132*, 9230–9231.

(7) Wagnert, L.; Berg, A.; Saltsman, I.; Gross, Z.; Rozenstein, V. J. *Phys. Chem. A* **2010**, *114*, 2059–2072.

(8) Lai, S.-L.; Wang, L.; Yang, C.; Chan, M.-Y.; Guan, X.; Kwok, C.-C.; Che, C.-M. *Adv. Funct. Mater.* **2014**, *24*, 4655–4665.

(9) (a) Thomas, K. E.; Alemayehu, A. B.; Conradie, J.; Beavers, C.; Ghosh, A. *Inorg. Chem.* **2011**, *50*, 12844–12851. (b) Rabinovich, E.; Goldberg, I.; Gross, Z. *Chem. - Eur. J.* **2011**, *17*, 12294–12301. (c) Thomas, K. E.; Beavers, C. M.; Ghosh, A. *Mol. Phys.* **2012**, *110*, 2439–2444. (d) Teo, R. D.; Gray, H. B.; Lim, P.; Termini, J.; Domeshek, E.; Gross, Z. *Chem. Commun.* **2014**, *50*, 13789–13792.

(10) Vestfrid, J.; Goldberg, I.; Gross, Z. *Inorg. Chem.* **2014**, *53*, 10536–10542.

(11) Shao, W.; Wang, H.; He, S.; Shi, L.; Peng, K.; Lin, Y.; Zhang, L.; Ji, L.; Liu, H. *J. Phys. Chem. B* **2012**, *116* (49), 14228–14233.

(12) Nardis, S.; Mandoj, F.; Paolesse, R.; Fronczek, F. R.; Smith, K. M.; Prodi, L.; Montalti, M.; Battistini, G. *Eur. J. Inorg. Chem.* **2007**, *2007*, 2345–2352.

(13) Wagnert, L.; Rubin, R.; Berg, A.; Mahammed, A.; Gross, Z.; Levanon, H. *J. Phys. Chem. B* **2010**, *114*, 14303–14308.

(14) Stensitzki, T.; Yang, Y.; Berg, A.; Mahammed, A.; Gross, Z.; Heyne, K. *Struct. Dyn.* **2016**, *3*, 043210.

(15) Lemon, C. M.; Halbach, R. L.; Huynh, M.; Nocera, D. G. *Inorg. Chem.* **2015**, *54*, 2713–2725.

(16) Vestfrid, J.; Botoshansky, M.; Palmer, J. H.; Durrell, A. C.; Gray, H. B.; Gross, Z. *J. Am. Chem. Soc.* **2011**, *133*, 12899–12901.

(17) Vestfrid, J.; Kothari, R.; Kostenko, A.; Goldberg, I.; Tumanskii, B.; Gross, Z. *Inorg. Chem.* **2016**, *55*, 6061–6067.

(18) Veracini, C. A.; Longeri, M.; Barili, P. L. *Chem. Phys. Lett.* **1973**, *19*, 592–595.

(19) Mertel, H. E. Halopyridines. In *Chemistry of Heterocyclic Compounds*; Klingsberg, E., Ed.; Interscience Publisher Inc.: London, 1961; Vol. 14, pp 299–419.

(20) Aronson, S.; Wilensky, S. B.; Yeh, T.-I.; Degraff, D.; Wieder, G. M. *Can. J. Chem.* **1986**, *64*, 2060–2063.

(21) Crystallography data deposited at the Cambridge Crystallographic Centre: (tpfc)Au, CCDC-1486464; (I<sub>4</sub>-tpfc)Cu, CCDC-1486466; (I<sub>4</sub>-tpfc)Ag, CCDC-1500821; (I<sub>4</sub>-tpfc)Au, CCDC-1500828.

(22) Liu, H.; Lai, T.; Yeung, L.; Chang, C. *Org. Lett.* **2003**, *5*, 617–620.

(23) Schechter, A.; Stanevsky, M.; Mahammed, A.; Gross, Z. *Inorg. Chem.* **2012**, *51*, 22–24.

(24) Golubkov, G.; Bendix, J.; Gray, H. B.; Mahammed, A.; Goldberg, I.; DiBilio, A. J.; Gross, Z. *Angew. Chem., Int. Ed.* **2001**, *40*, 2132–2134.

(25) Preuß, A.; Saltsman, I.; Mahammed, A.; Pfizner, M.; Goldberg, I.; Gross, Z.; Rö der, B. *J. Photochem. Photobiol., B* **2014**, *133*, 39–46.

(26) Egorov, S. Y.; Kamalov, V. F.; Koroteev, N. I.; Krasnovsky, A. A., Jr.; Toleutaev, B. N.; Zinukov, S. V. *Chem. Phys. Lett.* **1989**, *163*, 421–424.